A Novel Dual-mode Broadband Near-infrared Phosphor $Mg_5Ga_2Sn_2O_{12}$:Cr^{3+}, Ni^{2+} Designed Based on Energy Transfer Strategy

Xin Xie[a], Wanyin Ge[*a], Ye Tian[a], Maohao Yang[a], Yongxiang Li[b]

[a] School of Materials Science and Engineering, School of Antiquities Preservation Science & Technology, Shaanxi University of Science and Technology, Xi'an 710021, P. R. China

[b]School of Engineering, RMIT University, Melbourne, VIC 3000, Australia

* Corresponding author. Email: gewanyin@sust.edu.cn

Figures: 13

Tables: 3

Equations: 3

Figures:

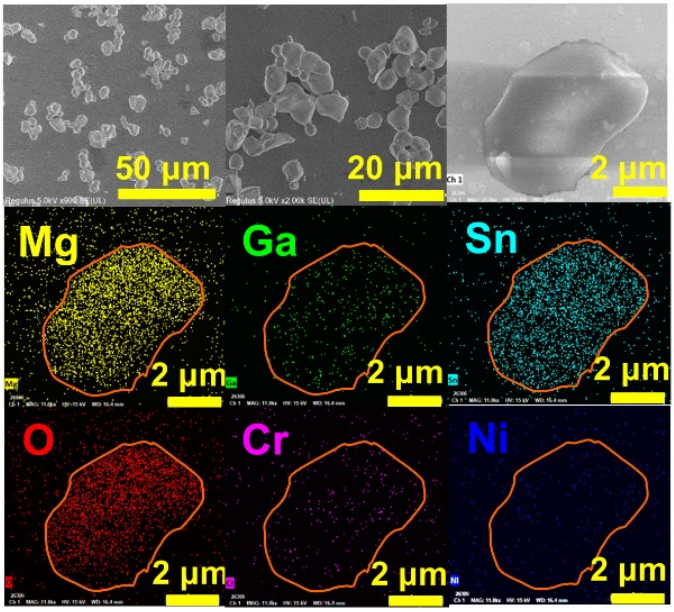

Fig. S1. SEM images and element distribution mappings of MGSO:0.1Cr^{3+}, 0.01Ni^{2+}.

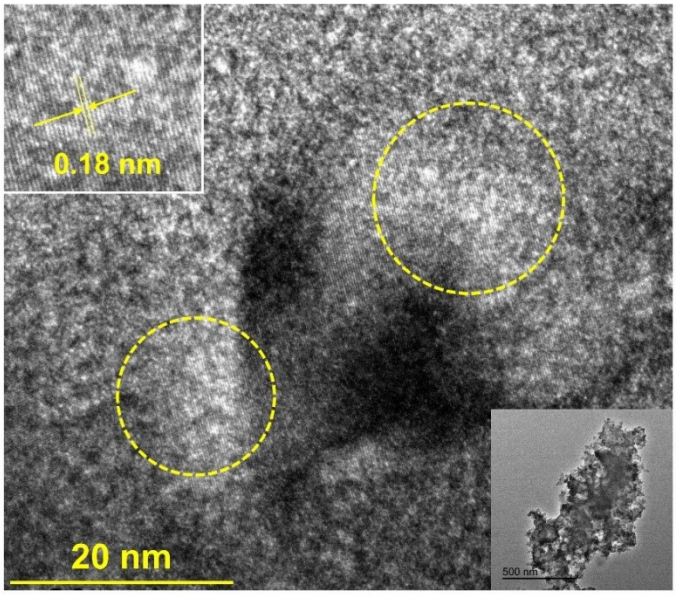

Fig. S2 TEM and HRTEM image of MGSO:0.1Cr^{3+}, 0.01Ni^{2+}.

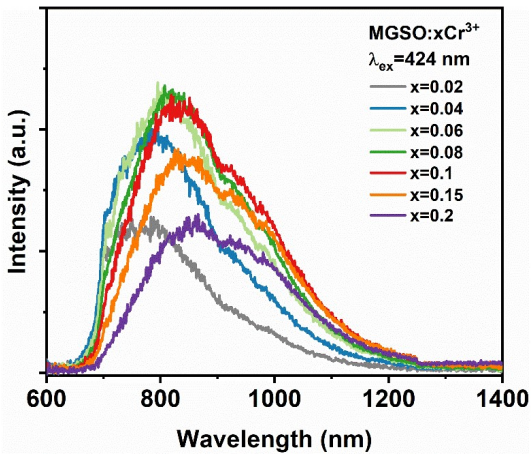

Fig. S3 PL spectra of MGSO:xCr^{3+}

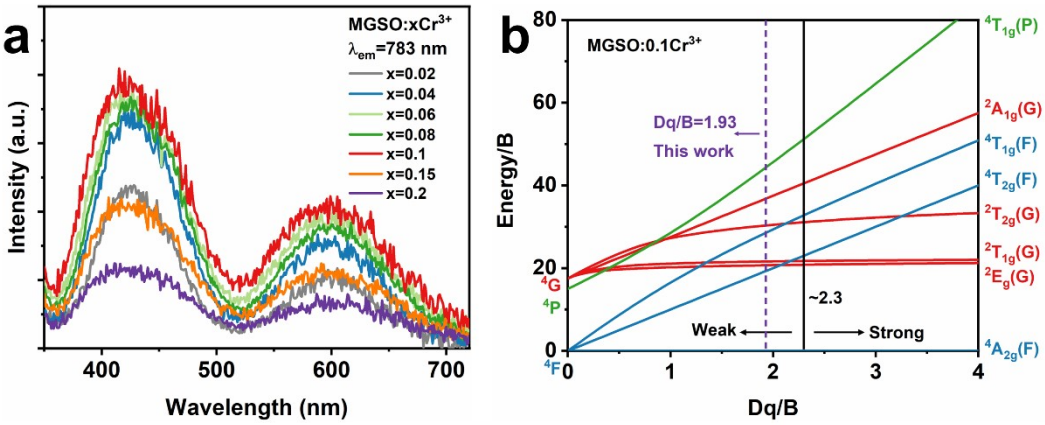

Fig. S4. (a) PLE spectra of MGSO:xCr^{3+}. (b) Tanabe-Sugano diagram of MGSO:0.1Cr^{3+}.

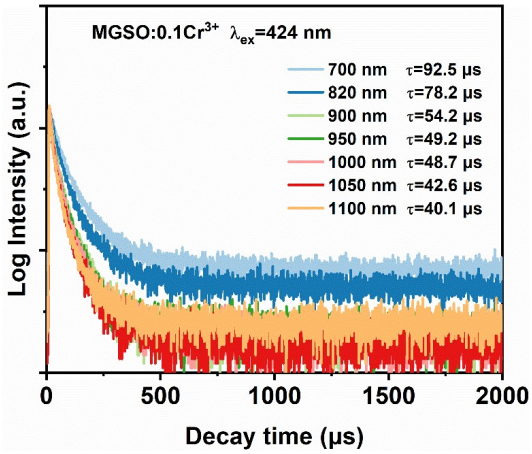

Fig. S5. Fluorescence decay curves of MGSO:0.1Cr^{3+} monitored at various emission wavelengths under 424 nm excitation.

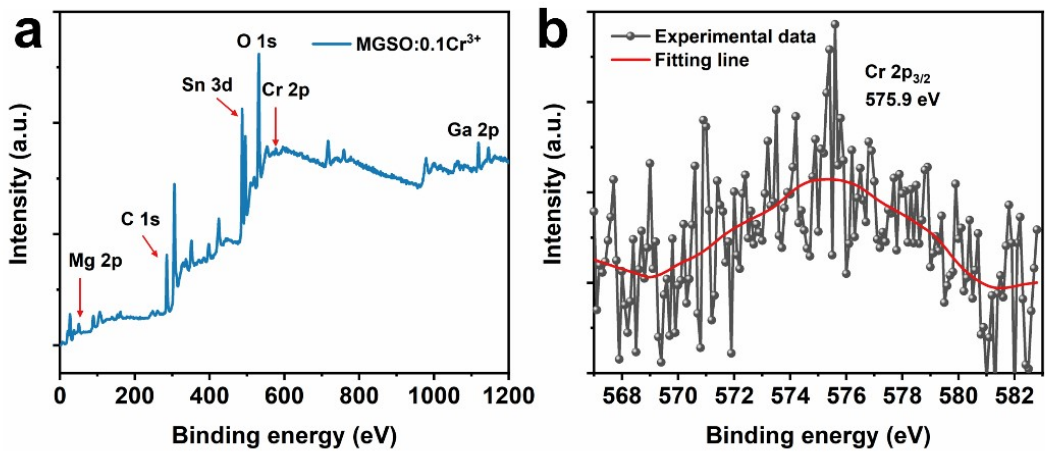

Fig. S6. (a) XPS spectrum of MGSO:0.1Cr^{3+}. (b) High-resolution XPS spectrum of Cr^{3+} for MGSO:0.1Cr^{3+}.

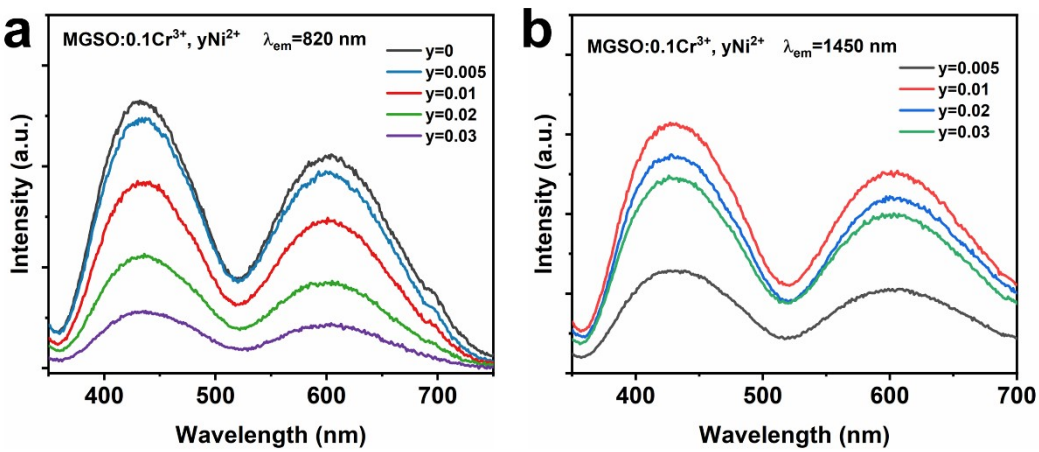

Fig. S7. (a) PLE spectra of MGSO:0.1Cr^{3+}, $y$$Ni^{2+}$ monitored at 820 nm. (b) PLE spectra of MGSO:0.1Cr^{3+}, $y$$Ni^{2+}$ monitored at 1450 nm.

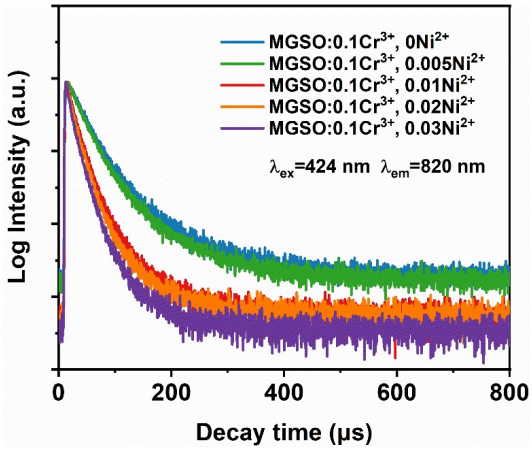

Fig. S8. Fluorescence decay curves of MGSO:0.1Cr^{3+}, $x$$Ni^{2+}$.

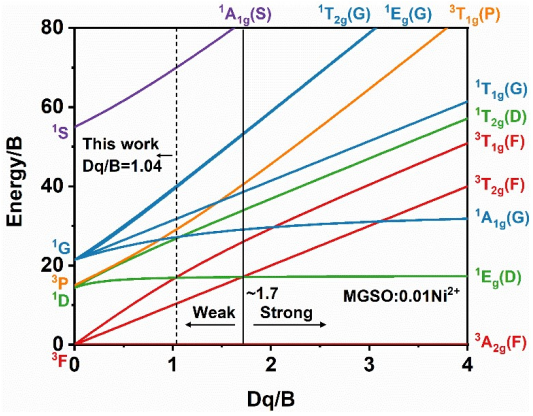

Fig. S9. Tanabe-Sugano diagram of MGSO:0.01Ni^{2+}.

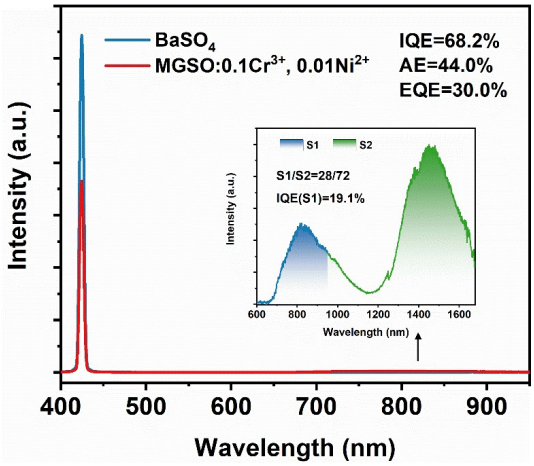

Fig. S10. Internal quantum efficiency and external quantum efficiency of MGSO:0.1Cr^{3+}, 0.01Ni^{2+}.

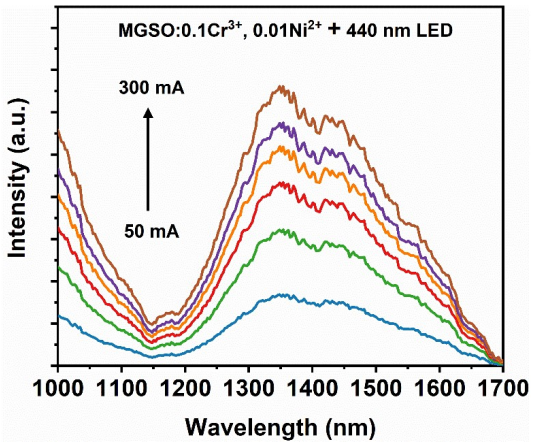

Fig. S11. Electroluminescence spectra of NIR-pc-LED.

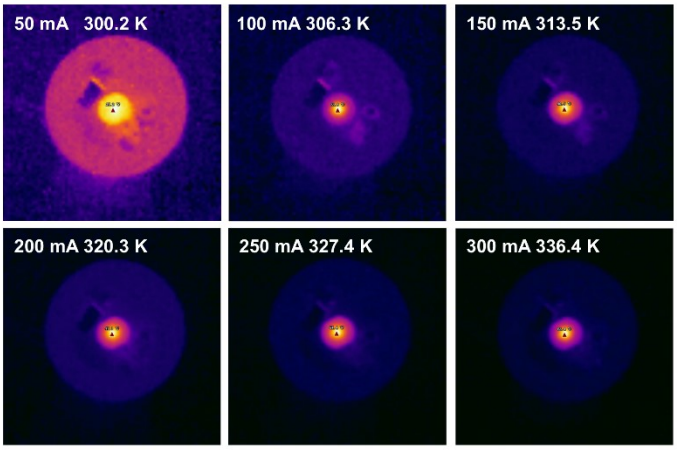

Fig. S12. Thermal imaging photos of NIR-pc-LED at different driving currents

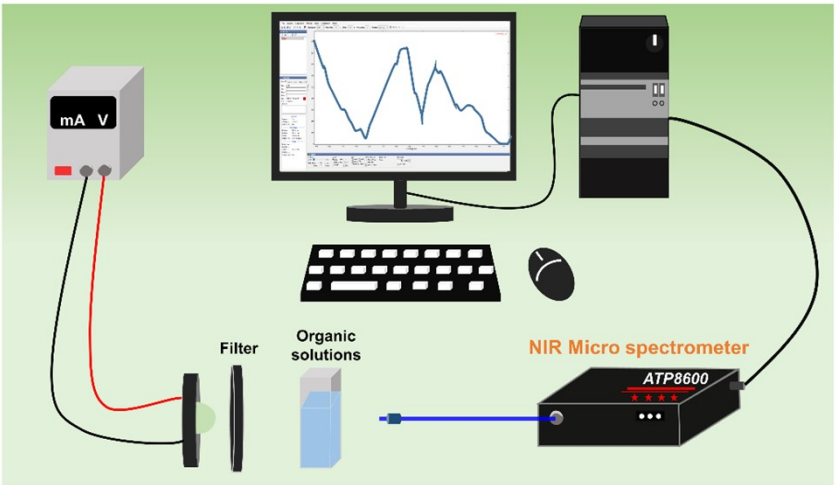

Fig. S13. Schematic diagram of using NIR-pc-LED for the non-destructive detection of organic solutions.

Tables:

Table S1 Rietveld refinement results of MGSO un-doped.

Sample	MGSO un-doped
Space group	*Fd*-3*m*（227）
Crystal structure	cubic
a (Å)	8.515
b (Å)	8.515
c (Å)	8.515
v (Å^3)	617.477
$\alpha=\beta=\gamma$ (°)	90
R_{wp}	15.46
R_p	11.57
χ^2	1.87

Table S2 Crystal field strength parameters of MGSO:xCr^{3+}.

MGSO:xCr^{3+}	0.02	0.04	0.06	0.08	0.1	0.15	0.2
Dq (cm^{-1})	1471.9	1462.5	1459.5	1449.2	1443.1	1447.7	1429.2
B (cm^{-1})	704.3	720.4	733.4	743.2	747.7	804.3	826.1
Dq/B	2.09	2.03	1.99	1.95	1.93	1.80	1.73

Table S3 Luminescence properties of several Ni2+-doped NIR phosphors.

Phosphors	λ_{ex} (nm)	λ_{em} (nm)	FWHM (nm)	IQE (%)	EQE (%)	Thermal stability(%)	Refs
$Ca_3Ga_2Ge_3O_{12}$:Cr^{3+},Ni^{2+}	450	1470	255	24.6	13.3	I_{385K}@50	1
La_2MgSnO_6:Mn^{4+},Ni^{2+}	365	1470	250	/	/	I_{398K}@43.1	2
$Mg_3Ga_2GeO_8$:Cr^{3+},Ni^{2+}	420	1425	300	62	18.1	I_{373K}@58.1	3
$Zn_3Ga_2GeO_8$:Cr^{3+},Ni^{2+}	410	1300	255	37.5	21.1	I_{360K}@27	4
$MgIn_2O_4$:Ni^{2+}	365	1520	311	47.93	34.66	I_{373K}@45	5
$Li_2ZnSn_3O_8$:Cr^{3+},Ni^{2+}	426	1465	300	43.31	18.24	I_{373K}@30.14	6
Ga_2O_3:Cr^{3+},Ni^{2+}	430	1460	300	53.5	21.2	I_{373K}@25.6	7
$Mg_7Ga_2GeO_{12}$:Cr^{3+},Ni^{2+}	448	1480	375	11.3	/	/	8
Mg_2SnO_4:Ni^{2+}	405	1480	297	21.6	4.9	I_{373K}@41.2	9
Ba_2MgWO_6:Ni^{2+}	365	1630	250	16.67	/	I_{423K}@50	10
$Mg_5Ga_2Sn_2O_{12}$:Cr^{3+},Ni^{2+}	424	1450	320	68.2	30	I_{383K}@38	This work

Equations:

The equations for calculating the crystal field strength parameter are as follows:[11]

$$10Dq = E\left({}^4T_2\right) = E\left({}^4A_2 \rightarrow {}^4T_2\right) - \frac{\Delta S}{2} \#(S1)$$

$$\frac{B}{Dq} = \frac{\left(\frac{\Delta E_{4T}}{Dq}\right)^2 - 10\left(\frac{\Delta E_{4T}}{Dq}\right)}{15\left(\frac{\Delta E_{4T}}{Dq} - 8\right)} \#(S2)$$

$$\Delta E_{4T} = E\left({}^4T_1\right) - E\left({}^4T_2\right) \#(S3)$$

where Dq represents the crystal field strength, B is the Rach parameter, ΔS is the Stokes shift, and ΔE_{4T} is the energy difference between the ${}^4A_2$ to ${}^4T_1$ and ${}^4T_2$ transitions.

References

1. F. Zhao, Y. Shao, Q. Liu and J. Zhong, Blue-light-excitable broadband $Ca_3Ga_2Ge_3O_{12}:Cr^{3+},Ni^{2+}$ phosphor for the applications in NIR-II window, *Laser Photonics Rev.*, 2024, **18**, 2400447.
2. Y. Liu, C. Dou, F. Dou, Z. Zhang, X. Gao, H. Zhang, S. Wang, X. Wang and H. Jiao, Enhanced NIR emission and thermal stability of $La_2MgSnO_6:Mn^{4+},Ni^{2+}$ via energy transfer, *J. Mater. Chem. C*, 2024, **12**, 13508-13515.
3. C. Wang, Y. Niu, Y. Wang, F. Wu, Q. Zhang, Y. Teng, H. Dong and Z. Mu, Multifunctional near-infrared phosphors Cr^{3+}/Ni^{2+} codoped $Mg_3Ga_2GeO_8$ based on energy transfer from Cr^{3+} to Ni^{2+}, *Inorg. Chem.*, 2024, **63**, 14383-14391.
4. L. Zheng, H. Wu, K. Zhao, Y. Liu, S. Wen, G. H. Pan, H. Wu, Z. Hao, L. Zhang and J. Zhang, Ultrabroadband near-infrared $Zn_3Ga_2GeO_8:Cr^{3+}$, Ni^{2+} phosphor for PiG pc-LED, *Adv. Opt. Mater.*, 2024, **12**, 2401521.
5. F. Zhu, Y. Deng, Y. Gao and J. Qiu, Long-wavelength near-infrared $MgIn_2O_4:Ni^{2+}$ phosphor with 47.93% IQE and 34.66% EQE for night vision lighting, nonvisual detection, and biological imaging, *ACS Materials Letters*, 2024, **6**, 4555-4563.
6. Z. Gao, Y. Zhang, Y. Li, S. Zhao, P. Zhang, X. Dong, D. Deng and S. Xu, Blue light-excited broadband NIR-II-emitting $Li_2ZnSn_3O_8:Cr^{3+},Ni^{2+}$ phosphor for multifunctional optical applications, *Inorg. Chem. Front.*, 2024, **11**, 4711-4720.
7. Y. Zhang, Z. Gao, Y. Li, H. Wang, S. Zhao, Y. Shen, D. Deng, S. Xu and H. Yu, Energy-transfer-enhanced Cr^{3+}/Ni^{2+} co-doped broadband near-infrared phosphor for fluorescence thermometers and near-infrared window imaging, *ACS Appl. Mater. Interfaces*, 2024, **16**, 57316-57324.
8. Y. Tang, P. Lyu, D. Yin, Z. Liu, N. Pan, K. Li, Y. Ye, C. Xu and L. Sun, Ultra-broadband emission from $Mg_7Ga_2GeO_{12}:Ni^{2+},Cr^{3+}$ phosphor spanning the NIR I–III regions for spectroscopy applications, *Materials Today Chemistry*, 2024, **42**, 102364.
9. B. M. Liu, X. X. Guo, L. Huang, R. F. Zhou, R. Zou, C. G. Ma and J. Wang, A super-broadband NIR dual-emitting $Mg_2SnO_4:Cr^{3+},Ni^{2+}$ phosphor for ratiometric phosphor-converted NIR light source applications, *Advanced Materials Technologies*, 2022, **8**, 2201181.
10. X. Lu, Y. Gao, J. Chen, M. Tan and J. Qiu, Long-wavelength near-infrared divalent nickel-activated double-perovskite Ba_2MgWO_6 phosphor as imaging for human fingers, *ACS Appl. Mater. Interfaces*, 2023, **15**, 39472-39479.
11. T. Liu, H. Cai, N. Mao, Z. Song and Q. Liu, Efficient near-infrared pyroxene phosphor $LiInGe_2O_6:Cr^{3+}$ for NIR spectroscopy application, *J. Am. Ceram. Soc.*, 2021, **104**, 4577-4584.